Title	Quantum impurity in the bulk of a topological insulator
Author(s)	Lu, H; Lu, H; Shen, S; Ng, T
Citation	Physics Reviews, 2013, v. 87, p. 195122
Issued Date	2013
URL	http://hdl.handle.net/10722/184650
Rights	Creative Commons: Attribution 3.0 Hong Kong License

Quantum impurity in the bulk of topological insulator

Hai-Feng Lü,[1,2] Hai-Zhou Lu,[1] Shun-Qing Shen,[1] and Tai-Kai Ng[3]

[1]*Department of Physics, The University of Hong Kong, Pokfulam Road, Hong Kong, China*
[2]*Department of Applied Physics, University of Electronic Science and Technology of China, Chengdu 610054, China*
[3]*Department of Physics, Hong Kong University of Science and Technology, Clear Water Bay Road, Hong Kong, China*

(Dated: May 21, 2013)

We investigate physical properties of an Anderson impurity embedded in the bulk of a topological insulator. The slave-boson mean-field approximation is used to account for the strong electron correlation at the impurity. Different from the results of a quantum impurity on the surface of a topological insulator, we find for the band-inverted case, that a Kondo resonant peak and in-gap bound states can be produced simultaneously. However, only one of them appears for the normal case. It is shown that the mixed-valence regime is much broader in the band-inverted case, while it shrinks to a very narrow regime in the normal case. Furthermore, a self-screening of the Kondo effect may appear when the interaction between the bound-state spin and impurity spin is taken into account.

PACS numbers: 71.27.+a, 73.20.Hb, 75.20.Hr

I. INTRODUCTION

A topological insulator (TI) is insulating in the bulk, but hosts conducting edge or surface states near the system boundary. It has attracted attention in the community of condensed matter physics due to its potential application in spintronics and quantum computation.[1–3] A class of materials such as Bi_2Se_3 and Bi_2Te_3 has been found to possess surface states which form a single Dirac cone.[4–6] Suppression of backscattering inside the Dirac cone guarantees that the Dirac dispersion remains essentially unperturbed for weak perturbation that preserves time-reversal symmetry.[7,8] So far, the effects of impurity scattering on the surface of TIs have been investigated extensively.[9–22] In the presence of classical spins which break time-reversal symmetry, it was predicted that the impurity could open up a local gap and suppress the local density of states.[9,10] The suppression of backscattering around nonmagnetic impurities on surfaces with strong spin-orbit coupling has been confirmed by scanning tunneling miscroscope experiments.[11–14] However, strong nonmagnetic scattering, such as that from electrostatic potentials, may disrupt the Dirac cone and create low-energy impurity resonances.[15] For a quantum impurity on the surface of a TI, the Hamiltonian for the impurity can be mapped to the conventional pseudo-gap Anderson model. The impurity is fully screened at low temperatures when the Fermi level is located away from the Dirac point.[16,17]

Although there are theoretical and experimental studies on the quasi-particle states around an impurity, most of them focus on the impurity on the surface of the TI. Essentially, the topological nature of TIs is determined by the electronic structure of the bulk bands instead of the surface states. On the other hand, the TI samples available nowadays are always poorly insulating in the bulk, owing to a large amount of vacancies and defects.[23–27] For these reasons, it is important to study how the quasiparticle states are affected when vacancies or impurities are localized in the bulk of the system. It has been shown that classical spins[18] or vacancies[19,20] localized in the bulk of TIs could result in the coexistence of in-gap bound states and boundary states. For a quantum impurity, the quantum fluctuations of its internal degree of freedom play an important role, making it significantly differ from classical impurities.[28] However, it remains unknown how a quantum impurity in the bulk of a TI affects the electronic states.

The study of quantum impurity in TIs is also related to the problems of impurities in unconventional density waves,[28–31] gapped systems,[32,33] or spin-orbit-coupled systems.[34–36] For instance, in a gapped system, the Kondo effect breaks down when the energy gap exceeds a critical value.[32] In the presence of Rashba spin-orbit interaction, a parity-breaking Dzyaloshinsky-Moriya term could be induced, resulting in a possible change of the Kondo temperature.[34–36] Since there are strong spin-orbit couplings and unconventional gaps in the TIs, it becomes interesting to investigate the differences between the Kondo effects in conventional insulators and TIs.

In this paper, we investigate the effects of a quantum impurity embedded in a TI with the help of the slave-boson mean-field approach. We show that in-gap bound states and Kondo effect could coexist in TIs, while only one of them appears for conventional insulators. If the bound states are singly occupied, the Kondo resonance could be screened by the exchange interaction between the impurity spin and the spin of the impurity-induced bound states, leading to a self-screened Kondo effect. The paper is organized as follows. In Sec. II we introduce a model Hamiltonian of an impurity in a TI and the slave-boson mean-field approach. In Sec. III we discuss the Kondo effect and the formation of the in-gap bound states in both band-inverted and normal cases. In Sec. IV, we show the self-screening of the Kondo effect. Finally, a summary is presented in Sec. V.

II. MODEL HAMILTONIAN AND SLAVE BOSON APPROACH

A. Model

The effective model to describe the bulk states of the TI with an impurity is written as

$$H = H_0 + H_d + H_t. \tag{1}$$

The part for the bulk electrons of TI is given by the modified Dirac model[37–39]

$$H_0 = \Psi_k^\dagger[\hbar v_F \vec{k}\cdot\vec{\alpha} + (mv_F^2 - B\hbar^2k^2)\beta]\Psi_k$$

with $\alpha_i = \sigma_x \otimes \sigma_i$ and $\beta = \sigma_z \otimes \sigma_0$, where σ_i $(i = x, y, z)$ are the Pauli matrices and σ_0 is the 2×2 unit matrix. $k_i = -i\partial_i$ $(i = x, y, z)$ is the momentum operator, $k^2 = k_x^2 + k_y^2 + k_z^2$, and v_F and m have the dimensions of speed and mass, respectively. Different from the surface Hamiltonian, a quadratic correction in momentum $-B\hbar^2k^2$ and a gap term mv_F^2 are introduced in the bulk Hamiltonian. The sign of mB determines whether the system is topologically trivial or not: it is nontrivial for $mB > 0$ (i.e., the band-inverted case), and trivial for $mB < 0$ (i.e., the normal case).[37–39] The energy spectra have a finite energy gap. Here the basis vectors are chosen as

$$\Psi_k^\dagger = \left(a_{k\uparrow}^\dagger, a_{k\downarrow}^\dagger, b_{k\uparrow}^\dagger, b_{k\downarrow}^\dagger\right),$$

where $a_{k\sigma}^\dagger$ and $b_{k\sigma}^\dagger$ are creation operators of electrons with spin σ on two different orbits. In this representation, we can rewrite the total Hamiltonian in the second-quantized form

$$\begin{aligned} H_0 &= \sum_{k\sigma}(mv_F^2 - B\hbar^2k^2)(a_{k\sigma}^\dagger a_{k\sigma} - b_{k\sigma}^\dagger b_{k\sigma}) \\ &+\hbar v_F \sum_k [k_z(a_{k\uparrow}^\dagger b_{k\uparrow} - a_{k\downarrow}^\dagger b_{k\downarrow}) \\ &+(k_x - ik_y)(a_{k\uparrow}^\dagger b_{k\downarrow} + b_{k\uparrow}^\dagger a_{k\downarrow}) + \text{H.c.}]. \end{aligned} \tag{2}$$

The Hamiltonian that describes the Anderson impurity is

$$H_d = \epsilon_d(c_{d\uparrow}^\dagger c_{d\uparrow} + c_{d\downarrow}^\dagger c_{d\downarrow}) + U c_{d\uparrow}^\dagger c_{d\uparrow} c_{d\downarrow}^\dagger c_{d\downarrow}, \tag{3}$$

where ϵ_d is the impurity energy level and U is the on-site Coulomb interaction. The coupling Hamiltonian between the impurity and electrons in TI has the form

$$H_t = \sum_{k\sigma}(V_{ak} a_{k\sigma}^\dagger c_{d\sigma} + V_{bk} b_{k\sigma}^\dagger c_{d\sigma} + \text{H.c.}), \tag{4}$$

where $V_{a(b)k}$ represents the overlap or hybridization matrix element between the magnetic impurity and conduction electrons in two bands.

B. Slave-boson mean field

Here we consider a strong on-site Coulomb interaction on the impurity, i.e., $U \to \infty$. In this limit, no double occupancy on the impurity is allowed. We introduce the auxiliary fields

$$c_{d\sigma}^\dagger = d_\sigma^\dagger b, c_{d\sigma} = b^\dagger d_\sigma,$$

where the boson operator $b^\dagger$ creates an empty state and the fermion operator $d_\sigma^\dagger$ creates a singly occupied state on the impurity. These two fields obey the local constraint $b^\dagger b + \sum_\sigma d^\dagger d = 1$.[40] In the mean-field approximation, both the annihilation and creation boson operators b and $b^\dagger$ are replaced by a complex number b_0 and its complex conjugate b_0^*, and the local constraint is realized by introducing a Lagrangian multiplier λ_0. Substituting the auxiliary fields in the original Hamiltonians (3) and (4), one can get

$$H_d = \tilde{\epsilon}_d(d_\uparrow^\dagger d_\uparrow + d_\downarrow^\dagger d_\downarrow) + \lambda_0(b_0^2 - 1)$$

and

$$H_t = \sum_{k\sigma}(\tilde{V}_{ak} a_{k\sigma}^\dagger d_\sigma + \tilde{V}_{bk} b_{k\sigma}^\dagger d_\sigma + \text{H.c.})$$

with the renormalized parameters $\tilde{\epsilon}_d = \epsilon_d + \lambda_0$ and $\tilde{V}_{a(b)k} = b_0 V_{a(b)k}$. The slave-boson mean-field approximation was first introduced to describe the low-energy physics of the conventional Anderson impurity model in the mixed-valence regime.[41] This method may produce the low-energy physics in unconventional density-waves (e.g., d-wave superconductors,[42] graphene electron systems,[43] etc.).

C. Green's functions

Utilizing the method of the equation of motion for the impurity electron, one finally obtains the retarded Green's function of the impurity electron,

$$\langle\langle d_\sigma | d_\sigma^\dagger \rangle\rangle = \frac{\omega - \tilde{\epsilon}_d - \Sigma_0(\omega) + \sigma\Sigma_z(\omega)}{[\omega - \tilde{\epsilon}_d - \Sigma_0(\omega)]^2 - \sum_i [\Sigma_i(\omega)]^2}, \tag{5}$$

where the self-energy functions are defined as

$$\begin{aligned} \Sigma_0(\omega) &= \sum_k \frac{(\omega + A_k)\tilde{V}_{ak}^2 + (\omega - A_k)\tilde{V}_{bk}^2}{\omega^2 - \hbar^2 v_F^2 k^2 - A_k^2}, \\ \Sigma_i(\omega) &= \sum_k \frac{2\hbar v_F k_i \tilde{V}_{ak}\tilde{V}_{bk}}{\omega^2 - \hbar^2 v_F^2 k^2 - A_k^2}, \end{aligned} \tag{6}$$

$(i = x, y, z)$, and $A_k = mv_F^2 - B\hbar^2k^2$.

It is assumed that the hybridization strength $V_{a(b)k}$ does not depend on momentum, $V_{a(b)k} = V_{a(b)}$. In the

absence of an external magnetic field, the interaction self-energy $\Sigma_i(\omega) = 0$ and the electronic Green's function can be simplified as

$$\langle\langle d_\sigma | d_\sigma^\dagger \rangle\rangle = \frac{1}{\omega - \tilde{\epsilon}_d - \Sigma_0(\omega)}, \quad (7)$$

which has the same form as those of the conventional Anderson impurity model. Additionally, we consider the case that the impurity is symmetrically coupled with two orbits, i.e., $V_0 = V_a = V_b$, and the self-energy $\Sigma_0(\omega)$ in d-dimensions ($d = 2, 3$) is thus simplified as

$$\begin{aligned}\Sigma_0(\omega) &= \omega \sum_k \frac{2\tilde{V}_0^2}{\omega^2 - \hbar^2 v_F^2 k^2 - A_k^2} \\ &= \frac{d\omega \tilde{V}_0^2 N_0}{k_F^d} \int_0^\infty dk \frac{k^{d-1}}{\omega^2 - \hbar^2 v_F^2 k^2 - A_k^2}, \quad (8)\end{aligned}$$

where N_0 is the number of lattice sites and k_F is the Fermi wave vector for the bulk of a TI.

D. Normal and band-inverted regimes

From the poles of self-energy function $\Sigma_0(\omega)$, one obtains the energy spectrum of the bulk,

$$\xi(k) = \pm\sqrt{\hbar^2 v_F^2 k^2 + (m v_F^2 - B\hbar^2 k^2)^2}.$$

The energy spectrum shows a complex dependence on the energy gap and momentum. Such energy spectra can be mapped onto many important cases of impurity problems. Near the band edges, the model reduces to the Anderson problem in normal insulators or semiconductors.[32,33] The quantum impurity model in graphene or surface states of the TIs can be recovered by setting $m = 0$ and $B = 0$.[16,17,22,43]

In Fig. 1 we present the energy spectra as a function of k for different values of mB. It can be seen from the energy spectrum that, for $mB < 1/2$, the band edges are located at $k = 0$ and the energy gap is

$$\Delta_N \equiv 2|m|v_F^2$$

as in normal insulators. However, for the case of $mB > 1/2$, the band edges appear at a finite k with a gap

$$\Delta_I \equiv \frac{\sqrt{4mB-1}}{|B|} v_F^2.$$

For convenience, one defines

$$g_0(\epsilon) = \frac{dN_0\tilde{V}_0^2\epsilon\left[\sqrt{\epsilon^2 - \Delta_I^2/4} - \frac{1-2mB}{2|B|}v_F^2\right]^{\frac{d-2}{2}}}{4(|B|\hbar^2 k_F^2)^{\frac{d}{2}}\sqrt{\epsilon^2 - \Delta_I^2/4}} \quad (9)$$

when $\epsilon > \Delta_N/2$, and

$$g_1(\epsilon) = \frac{dN_0\tilde{V}_0^2\epsilon\left[\sqrt{\epsilon^2 - \Delta_I^2/4} + \frac{2mB-1}{2|B|}v_F^2\right]^{\frac{d-2}{2}}}{4(|B|\hbar^2 k_F^2)^{\frac{d}{2}}\sqrt{\epsilon^2 - \Delta_I^2/4}} \quad (10)$$

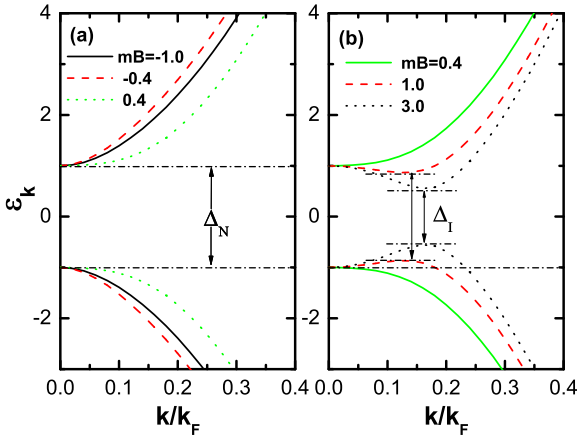

FIG. 1: The energy spectrum ϵ_k for different mB values: (a) $mB = -1.0, -0.4, 0.4$; (b) $mB = 0.4, 1.0, 3.0$. Here mv_F^2 is taken as the energy unit. For $mB < 1/2$, the energy gap is located at $k = 0$ and equals $\Delta_N \equiv 2|m|v_F^2$. For $mB > 1/2$, the energy gap is located at a finite k and equals $\Delta_I \equiv \frac{\sqrt{4mB-1}}{|B|}v_F^2$.

when both $\Delta_I/2 < \epsilon < \Delta_N/2$ and $mB > 1/2$ are satisfied.

For the case of $mB < 1/2$, one gets

$$\Sigma_0(\omega) = \int_{\frac{\Delta_N}{2}}^\infty d\xi g_0(\xi)\left[\frac{1}{\omega - \xi} + \frac{1}{\omega + \xi}\right]. \quad (11)$$

After analytical continuation, $\Sigma_0(\omega) = \mathrm{Re}\Sigma_0(\omega) + \mathrm{Im}\Sigma_0(\omega)$ with

$$\mathrm{Re}\Sigma_0(\omega) = \mathrm{P}\int_{\frac{\Delta_N}{2}}^\infty d\xi g_0(\xi)\left[\frac{1}{\omega - \xi} + \frac{1}{\omega + \xi}\right] \quad (12)$$

and

$$\mathrm{Im}\Sigma_0(\omega) = -g_0(\omega)\Theta(|\omega| - \frac{\Delta_N}{2}) \quad (13)$$

with P denoting the principal value.

For the case of $mB > 1/2$, the real and imaginary parts of the self-energy are given by

$$\begin{aligned}\mathrm{Re}\Sigma_0(\omega) &= \mathrm{P}\left[\int_{\frac{\Delta_I}{2}}^{\frac{\Delta_N}{2}} d\xi g_2(\xi)\right. \\ &+ \left.\int_{\frac{\Delta_N}{2}}^\infty d\xi g_0(\xi)\right]\left(\frac{1}{\omega - \xi} + \frac{1}{\omega + \xi}\right) \quad (14)\end{aligned}$$

and

$$\begin{aligned}\mathrm{Im}\Sigma_0(\omega) &= -\left[g_2(\omega)\Theta(|\omega| - \frac{\Delta_I}{2})\Theta(\frac{\Delta_N}{2} - |\omega|)\right. \\ &+ \left. g_0(\omega)\Theta(|\omega| - \frac{\Delta_N}{2})\right], \quad (15)\end{aligned}$$

where $g_2(\omega) = g_0(\omega) + g_1(\omega)$. Because $\mathrm{Im}\Sigma_0$ is proportional to the density of states of the bulk electrons, the density of states is discontinuous at the point $\Delta_N/2$. For a relatively large B and small m, the energy gap reduces to a value much smaller than Δ_N.

The free energy F of the system is given by the partition function

$$F = -\frac{1}{\beta}\ln Z = -\frac{1}{\beta}\int_{-\infty}^{\infty} \ln(1+e^{-\beta(\omega-\mu)})\bar{\rho}(\omega)d\omega,$$

where $\bar{\rho}(\omega) = \Sigma_k \delta(\omega - \epsilon_k)$, ϵ_k are the one-electron energies of the system, μ is the chemical potential of the TI, and $\beta = 1/k_B T$ is the system temperature. $\bar{\rho}(\omega)$ can be calculated from the poles of the one-electron Green's function and is given by

$$\bar{\rho}(\omega) = \frac{\mathrm{Im}}{\pi}\sum_k \frac{4\omega}{\omega^2 - \hbar^2 v_F^2 k^2 - A_k^2} + 2\frac{\mathrm{Im}}{\pi}\frac{\partial}{\partial\omega}\ln\langle\langle d_\sigma | d_\sigma^\dagger\rangle\rangle.$$

Minimizing the free energy of the system with respect to λ_0 and b_0, one obtains a set of self-consistent equations

$$\begin{aligned} 2\int_{-\infty}^{\infty} d\omega f(\omega)\rho_d(\omega) + b_0^2 - 1 &= 0, \\ 2\int_{-\infty}^{\infty} d\omega f(\omega)(\omega - \tilde{\epsilon}_d)\rho_d(\omega) + \lambda_0 b_0^2 &= 0, \end{aligned} \qquad (16)$$

where $f(\omega) = [1+e^{(\omega-\mu)/k_B T}]^{-1}$ is the Fermi distribution function and the density of states $\rho_d(\omega)$ of the impurity is given by

$$\rho_d(\omega) = -\frac{1}{\pi}\frac{\mathrm{Im}\Sigma_0(\omega)}{[\omega - \tilde{\epsilon}_d - \mathrm{Re}\Sigma_0(\omega)]^2 + \mathrm{Im}\Sigma_0(\omega)^2}.$$

In the calculation, it is limited to zero temperature, i.e., $k_B T = 0$. $\Delta_N/2$ is taken as the energy unit and $\Gamma_0 = \pi\rho_0 V_0^2$ represents the hybridization strength between the impurity and the bulk electrons, where $\rho_0 = N_0/2D$ is the density of states per spin at the chemical potential and $D = \sqrt{(\hbar v_F k_F)^2 + (m v_F^2 - B\hbar^2 k_F^2)^2}$ is a cut-off of the band width. In the following, we show the results of quantum impurity in three-dimensional TIs for $\Gamma_0 = 0.5$ and $D = 30.0$.

III. IN-GAP BOUND STATES AND THE KONDO EFFECT

A. Self-energy

First, we discuss the self-energy $\Sigma_0(\omega)$, which depends on the energy spectrum of the bulk bands. In the bulk of the TI, the strong spin-orbit coupling couples the conduction and valence bands, leading to the non-parabolic energy spectrum. The self-energy $\Sigma_0(\omega)$ reveals not only the poles of the Green's function, but also the inhomogeneous density of states due to the impurity-induced states.

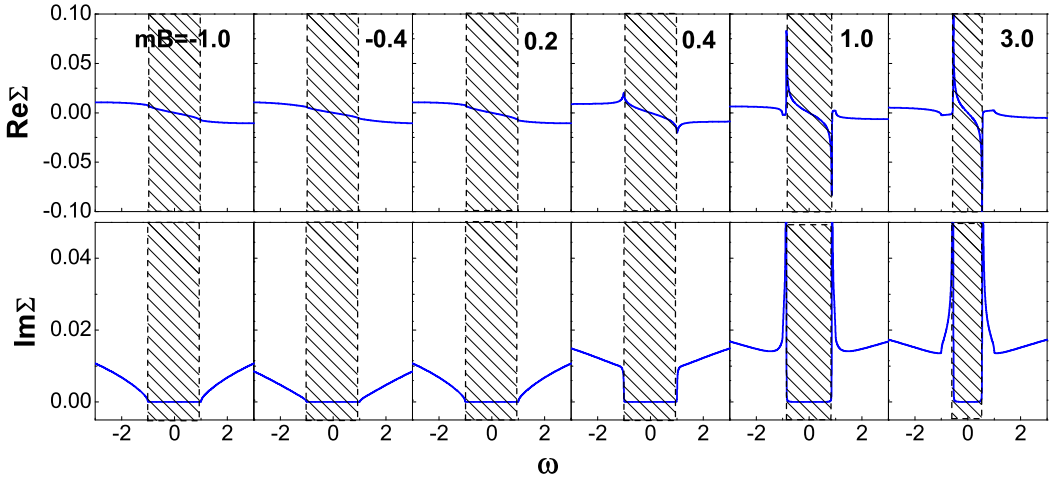

FIG. 2: The real and imaginary parts of the self-energy $\Sigma_0(\omega)$ for different mB values. The shaded part represents the region of energy gap.

Figure 2 shows the real and imaginary parts of $\Sigma_0(\omega)$ versus ω for different values of mB. Previous studies based on the Chern number and Z_2 invariant indicate

that the band-inverted case with $mB > 0$ is topologically nontrivial, while the normal case with $mB < 0$ is topologically trivial.[37–39] It is shown that in Fig. 2 both the real and imaginary parts of $\Sigma_0(\omega)$ are quite different for opposite signs of mB. The real part $\mathrm{Re}\Sigma_0(\omega)$ determines the level positions of both the Kondo resonance and the bound states, according to the solutions to the equation

$$\omega = \tilde{\epsilon}_d + \mathrm{Re}\Sigma_0(\omega). \tag{17}$$

For $mB > 1/2$, $\mathrm{Re}\Sigma_0(\omega)$ diverges rapidly near the edges of the gap, thus there always exist bound states within the gap. When the impurity level $|\epsilon_d|$ is much larger than $\Delta_I/2$, the bound states are very close to the bottom of the conduction bands for $\epsilon_d \gg \Delta_I/2$ or the top of the valence band for $\epsilon_d \ll -\Delta_I/2$, which is similar to the case of s-wave superconductors.[44] More importantly, Eq. (17) has an extra solution in the band region, corresponding to the coexisting Kondo resonance. For $mB < 0$, there is only one solution to Eq. (17), so the Kondo effect and the bound states do not appear simultaneously.

The imaginary part $\mathrm{Im}\Sigma_0(\omega)$ is proportional to the density of states of bulk electrons. For $mB > 1/2$, the energy gap is Δ_I, thus $\mathrm{Im}\Sigma_0(\omega) = 0$ in the region of $\omega \in [-\Delta_I/2, \Delta_I/2]$. At the band edges $\pm\Delta_I/2$, $\mathrm{Im}\Sigma_0(\omega)$ shows divergences. In the region $|\omega| \in [\Delta_I/2, \Delta_N/2]$, the divergences drops rapidly with the increasing $|\omega|$. For $|\omega| > \Delta_N/2$, $\mathrm{Im}\Sigma_0(\omega)$ begins to increase as a function of $\sqrt{\omega}$. For $0 < mB < 1/2$, the divergences at the band edges $\pm\Delta_N/2$ disappear gradually with decreasing mB. For $mB < 0$, $\mathrm{Im}\Sigma_0(\omega)$ at the band edges is always zero and increases as a function of $\sqrt{\omega}$ for $|\omega| > \Delta_N/2$.

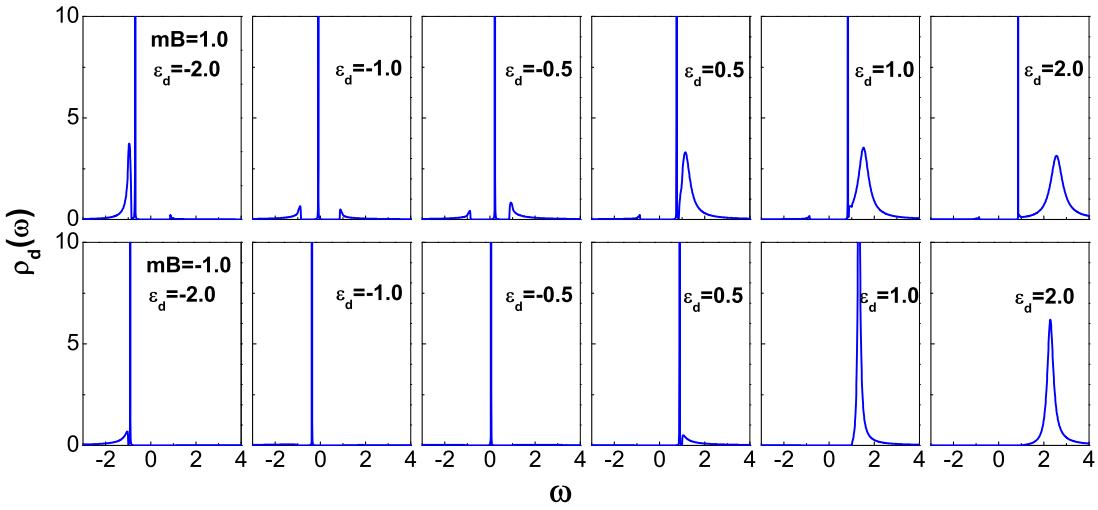

FIG. 3: The density of states of the impurity electron is shown for different impurity levels $\epsilon_d = -2.0$, -1.0, -0.5, 0.5, 1.0, and 2.0 (from left to right) in (a) topological nontrivial case $mB = 1.0$ and (b) topological trivial case $mB = -1.0$, where the chemical potential $\mu = 0.0$ lies in the gap.

B. Density of states of the impurity

From the self-energy, the Kondo resonance and the bound states have been discussed qualitatively. The density of states $\rho_d(\omega)$ of the impurity for the cases that the chemical potential μ lies in the gap and in the valence bands are presented in Figs. 3 and 4, respectively. It is demonstrated that in both cases the Kondo resonance and bound states coexist for $mB > 0$, while only one of them appears for $mB < 0$. For $mB > 0$, the bound states are very close to the band edges when $\tilde{\epsilon}_d$ is far away from the energy gap. In the previous studies,[31–33] it has been argued that when the energy gap exceeded an critical value ($\Delta/T_K = 2.0$ predicted by slave-boson mean-field theory[32] and T_K is the Kondo temperature), the Kondo effect no longer appears in the insulators with an energy-independent density of states. However, for a complex dispersion relation, the density of states is strongly energy-resolved and quite different near the band edges for the band-inverted and normal cases. In the band-inverted case, $\rho_d(\pm\Delta_I/2)$ equals zero exactly, due to the divergence of $\mathrm{Im}\Sigma_0(\omega)$ near the band edges.

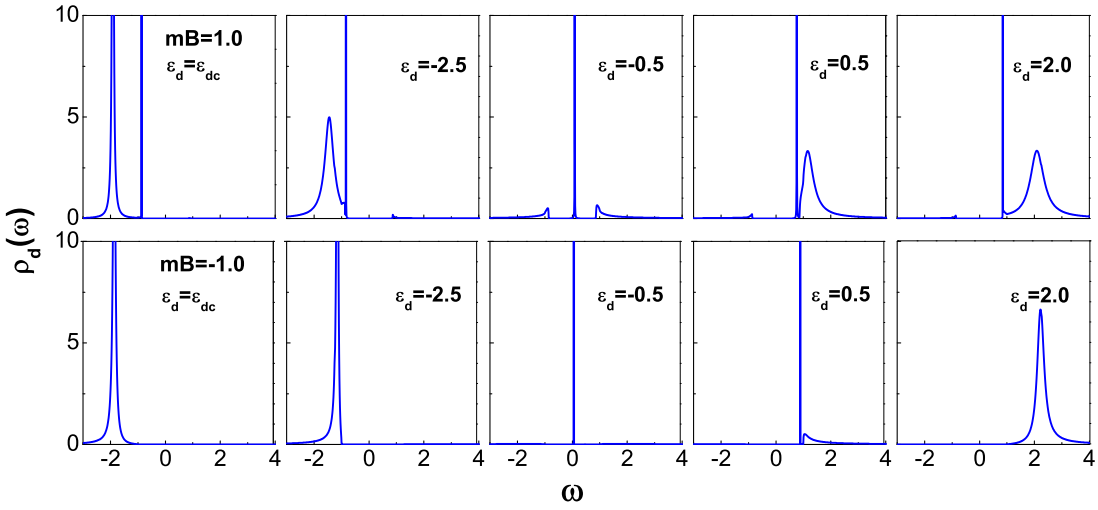

FIG. 4: The density of states of the impurity electron is shown for different impurity levels $\epsilon_d = \epsilon_{dc}$ (ϵ_{dc} is the critical point at which $\tilde{\epsilon}_d = \mu$), -2.5, -0.5, 0.5, and 2.0 (from left to right) in (a) topological nontrivial case $mB = 1.0$ and (b) topological trivial case $mB = -1.0$, where the chemical potential $\mu = -2.0$ lies in the valence band.

For $|\omega| \gg \Delta_I$, $\rho_d(\omega)$ also approaches zero. Therefore, no matter how μ lies in the gap or in the bands, there are always two low-energy resonance peaks lying near the band edges for $mB > 1/2$, as shown in the upper panels of Figs. 3 and 4. When the chemical potential μ lies in the valence band, the low-energy resonance peak becomes narrow and its position moves to μ with decreasing ϵ_d. Near the critical point ϵ_{dc}, the resonance peak becomes very sharp and close to the chemical potential.

In Fig. 5 we present the positions of the in-gap bound states and low-energy Kondo resonance as functions of the impurity level ϵ_d in the normal and band-inverted cases. The bound states show quite different behaviors in the two cases. For the normal case, the position of the bound states is almost linear in ϵ_d. The in-gap bound states start from the point $\epsilon_{dc} = -\Delta_N/2$, corresponding to the top of the valence bands. At the bottom of the conduction bands, the bound states enter the conduction bands continuously, and then the low-energy Kondo resonance peak appears. However, for the band-inverted case, the bound states in the gap and the Kondo resonance can form simultaneously for the impurity level $\epsilon_d > \epsilon_{dc}$. In this case, the positions of these two states do not connect at any point. For an ϵ_d far away from the chemical potential, the in-gap bound states are very close to the band edges. Thus they are vulnerable to small perturbation or thermal fluctuation, and may merge into the conduction bands easily.

Above we demonstrate that the presence of the in-gap bound states is determined by the topological nature of the TI. For real TI materials such as Bi_2Se_3 and Bi_2Te_3, the system parameters from first principles calculations[4] are $(mv_F^2, \hbar v_F, B) = (0.28\text{eV}, 3.2\text{eV\AA}, 33\text{eV\AA}^2)$ and $(0.30\text{eV}, 2.9\text{eV\AA}, 57\text{eV\AA}^2)$, respectively. Correspondingly, $mB \sim 0.9$ for Bi_2Se_3 and 2.0 for Bi_2Te_3. Therefore, it is expected that the coexistence of in-gap bound state and Kondo effect could be observed in these two materials.

C. Broadened mixed-valence regime for band-inverted case

The mean field b_0^2 introduced in Sec. II B gives the probability that the impurity is empty. Figure 6 presents the dependence of b_0^2 on the impurity energy level ϵ_d for different values of mB. $b_0^2 = 0$ when the impurity level ϵ_d is much lower than the chemical potential, which means that the impurity is singly occupied. In this case, the charge fluctuation between the impurity and the bulk bands is suppressed. When ϵ_d exceeds a threshold value, b_0^2 begins to increase from 0 and saturates at 1 when $\epsilon_d \gg \mu$. The mixed-valance regime is defined as where b_0^2 changes from 0 to 1. Figure 6 presents b^2 when the chemical potential lies in the gap and in the valence bands. As shown in Fig. 6, the mixed-valence regime is broader for the band-inverted case with $mB > 0$. For the normal case with $mB < 0$, b_0^2 increases more rapidly, and the mixed-valence regime shrinks into a very narrow regime. This kind of narrow mixed-valence regime has also been found in unconventional density waves and d-wave superconductors.[28,31] For $mB < 0$, the density of states of bulk electrons vanishes at the band edges. The reduction of the density of states at the band edges

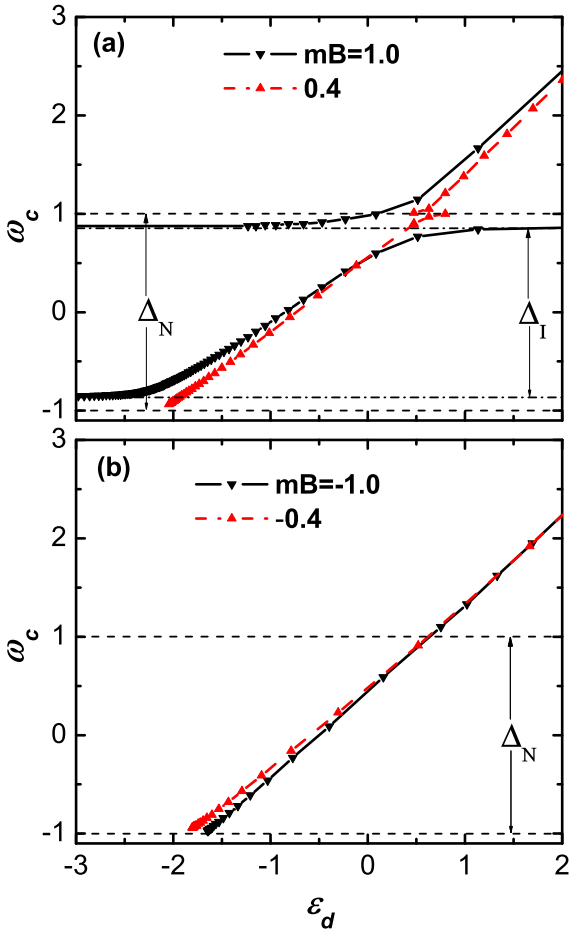

FIG. 5: The positions of the bound states and low-energy Kondo resonance peak as functions of impurity level ϵ_d in (a) the topological nontrivial case $mB = 1.0, 0.4$ and (b) the topological trivial case $mB = -1.0, -0.4$. The chemical potential is taken as $\mu = 0.0$.

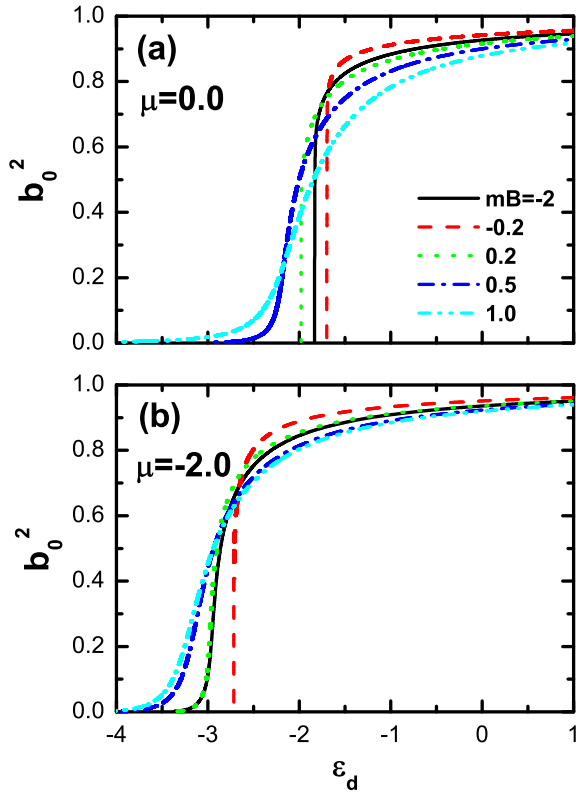

FIG. 6: The dependence of the order parameter b_0^2 on the impurity energy level ϵ_d for (a) the chemical potential in the gap $\mu = 0.0$ and (b) in the valence band $\mu = -2.0$. Here $mB = -2.0$ and -0.2 represent the topological nontrivial case and $mB = 0.2$, 0.5, and 1.0 correspond the topological trivial case.

implies that the Kondo resonance peak is narrower and b_0^2 decreases to zero faster than those in the conventional case. From the self-consistent equations, near the critical point, the critical value of ϵ_d is determined by

$$\epsilon_{dc} = 2\int_{-D}^{\mu} d\omega \frac{g(\omega)}{\omega - \tilde{\epsilon}_d},$$

where $g(\omega)$ is proportional to the density of states of the background electrons. In the band-inverted case, $g(\omega)$ diverges near the band edges, which results in a large integral value as well as large $|\epsilon_{dc}|$. In contrast, $g(\omega)$ reduces to zero near the band edges in the normal case. In this case, $|\epsilon_{dc}|$ is smaller and the mixed-valence regime becomes narrower.

D. In two dimensions

The preceding sections present the numerical results in three dimensions. In this section, we briefly discuss the behaviors of the quantum impurity in the bulk of two-dimensional TIs. In practice, the two-dimensional case is more accessible by the scanning tunneling miscroscope.[14] At the mean-field level, the difference between two and three dimensions arises from the self-energy $\Sigma_0(\omega)$, which in two dimensions can be expressed as

$$\Sigma_0(\omega) = \frac{2\omega \tilde{V}_0^2 N_0}{k_F^d} \int_0^{\infty} dk \frac{k}{\omega^2 - \hbar^2 v_F^2 k^2 - A_k^2}.$$

A detailed discussion about the properties of $\Sigma_0(\omega)$ in two dimensions is presented in Ref. 45, in which a δ-impurity scattering is considered. It can be deduced that, at the point $\omega = \Delta_N/2$, the self-energy $\Sigma_0(\omega)$ is finite in three dimensions, while in two dimensions, $\Sigma_0(\omega)$ has logarithmic divergence to $-(+)\infty$ at $\omega \to +(-)|m|$ for TIs and has logarithmic divergence to $+(-)\infty$ at

$\omega \to -(+)|m|$ for normal insulators.[45] This means that, when the Anderson impurity couples only to one band, the topological phase transition can be seen from the position of impurity bound states as the system changes from normal insulator to TI. Besides, the physical properties of the quantum impurity are similar qualitatively in two and three dimensions, e.g., the mixed-valence regime in both cases is much broader for $mB > 0$ than the case of $mB < 0$.

IV. SELF-SCREENING OF THE KONDO EFFECT

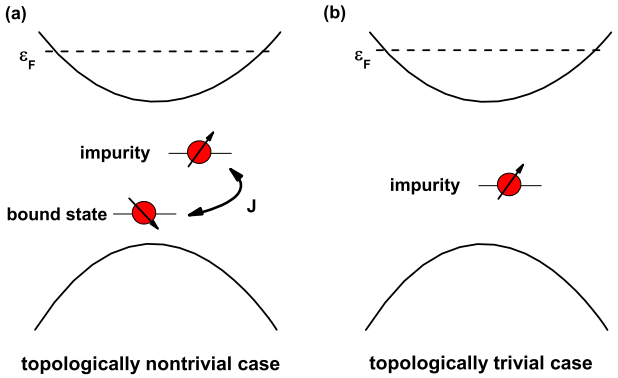

FIG. 7: Illustration of the Kondo effect for (a) topological nontrivial case and (b) trivial case.

We have shown that the quantum impurity may induce in-gap bound states in the band-inverted case, leading to the coexistence of the Kondo resonance and the bound states. This indicates that the Kondo resonance and bound state originate from two different mechanisms. The singly-occupied quantum impurity behaves like a single spin, and gives the Kondo resonance when the system is in the Kondo regime. The bound state, on the other hand, is induced when the system is topologically nontrivial. Even a potential scattering[18] or a vacancy[19] could produce the in-gap bound state in the bulk of TIs. Therefore, the in-gap bound state could be considered as a degree of freedom, while its energy is determined by the impurity. When the chemical potential of the TI lies in the conduction bands, both the bound states and the impurity level are occupied, and each of them behaves like a single localized spin (as illustrated in Fig. 7). It is quite naturally to expect the exchange interaction between two quantum spins, which is usually due to second-order virtual hopping or the Ruderman-Kittel-Kasuya-Yosida (RKKY) mechanism mediated by itinerant electrons. If the interaction is antiferromagnetic, the two spins form a singlet, which will compete with the many-body singlet formed by the impurity spin and conduction electrons, quenching their Kondo effect. Different from the intensively studied two-impurity Kondo problem,[46,47] here the quenched Kondo effect is induced by the spin of the bound states rendered by the impurity itself. Therefore, we refer to this effect as the self-screening of the Kondo effect.

A. Exchange interaction between impurity spin and impurity-induced bound-state spin

The self-screened Kondo effect can be illustrated by the model Hamiltonian as follows

$$\begin{aligned} H &= H_0 + \sum_\sigma \epsilon_d d^\dagger_\sigma d_\sigma + \sum_\sigma \epsilon_f f^\dagger_\sigma f_\sigma + J\mathbf{S}_d \cdot \mathbf{S}_f \\ &+ \sum_{k\sigma} (V_d b_d a^\dagger_{k\sigma} d_\sigma + V_d b_d b^\dagger_{k\sigma} d_\sigma + \text{H.c.}) \\ &+ \sum_{k\sigma} (V_f b_f a^\dagger_{k\sigma} f_\sigma + V_f b_f b^\dagger_{k\sigma} f_\sigma + \text{H.c.}) \\ &+ \lambda_d (\sum_\sigma d^\dagger_\sigma d_\sigma + b_d^2 - 1) + \lambda_f (\sum_\sigma f^\dagger_\sigma f_\sigma + b_f^2 - 1), \end{aligned} \tag{18}$$

where ϵ_f is the impurity-induced bound-state level and H_0 is the Hamiltonian for the bulk of the TI [Eq. (2)]. The term $J\mathbf{S}_d \cdot \mathbf{S}_f$ describes the exchange interaction between the impurity spin and bound-state spin. It is noted that here the quantum impurity and its induced in-gap bound state are considered as two degrees of freedom.

The above effective Hamiltonian describes the low-energy behavior of the Anderson impurity in the nontrivial TI phase of the system. It can be derived from a renormalization-group approach where the high-energy degree of the system is integrated out systematically. The derivation of the effective coupling between the bound state and Kondo resonance requires a technique beyond the slave-boson mean-field theory, which was presented recently.[48] Using a weak coupling renormalization group analysis, it has been shown that the exchange interaction J between the d and induced f spins may be renormalized dynamically to either positive or negative values. In the regime where charge fluctuations in both d and f states are quenched, the system is in the self-screened Kondo regime for $J > 0$ and in the SO(3) Kondo regime for $J < 0$,[48] respectively. Here we introduce the exchange interaction J and perform the slave-boson approach to describe the Kondo physics for small charge fluctuations in the regime of $J > 0$.

B. Order parameter for the exchange interaction

Similar to the treatment in Sec. II B, two slave-boson operators b_d and b_f are introduced to replace $c_{d(f)\sigma}$ by $b^\dagger_{d(f)} d(f)_\sigma$ in the large-U limit. The spin exchange term $J\mathbf{S}_d \cdot \mathbf{S}_f = J\sum_{\sigma,\sigma'} d^\dagger_\sigma d_{\sigma'} f^\dagger_{\sigma'} f_\sigma$ can be decoupled by introducing a valence-bond field $\Delta_0 = -\sum_\sigma \langle d^\dagger_\sigma f_\sigma \rangle$. In the

mean-field approximation[47]

$$J\mathbf{S}_d\cdot\mathbf{S}_f\to J\Delta_0\sum_\sigma(d_\sigma^\dagger f_\sigma+f_\sigma^\dagger d_\sigma)+J\Delta_0^2,$$

the Hamiltonian becomes quadratic in the fermion operators. The problem is still far from trivial as b_d, b_f, λ_d, λ_f, Δ_0, and ϵ_f need to be determined self-consistently. Different from the ordinary Kondo problem, here the bound-state energy ϵ_f also enters the self-consistent equations. By minimizing the ground-state energy, one obtains a set of nonlinear self-consistent equations

$$\begin{aligned}
\sum_\sigma\langle d_\sigma^\dagger d_\sigma\rangle+b_d^2-1 &= 0,\\
\sum_\sigma\langle f_\sigma^\dagger f_\sigma\rangle+b_f^2-1 &= 0,\\
\sum_\sigma(\langle d_\sigma^\dagger f_\sigma\rangle+\langle f_\sigma^\dagger d_\sigma\rangle)+2\Delta_0 &= 0,\\
\sum_{k,\sigma}(V_d\langle a_{k\sigma}^\dagger d_\sigma\rangle+V_d\langle b_{k\sigma}^\dagger d_\sigma\rangle+h.c.)+2b_d\lambda_d &= 0,\\
\sum_{k,\sigma}(V_f\langle a_{k\sigma}^\dagger f_\sigma\rangle+V_f\langle b_{k\sigma}^\dagger f_\sigma\rangle+h.c.)+2b_f\lambda_f &= 0.
\end{aligned}\tag{19}$$

To simplify the calculation, we assume that the bound states are always singly occupied ($b_f=0$) and decoupled from the conduction electrons. In this case, the in-gap bound states act like a single spin. Correspondingly, the constraints for the bound states becomes $\lambda_f(\sum_\sigma\langle f_\sigma^\dagger f_\sigma\rangle-1)$ and λ_f is contained in the related Green's functions.

C. Green's functions

Performing the equation of motion procedure, we can obtain the Green's functions for the impurity and the bound states,

$$\begin{aligned}
\langle\langle d_\sigma|d_\sigma^\dagger\rangle\rangle &= \frac{1}{\omega-\tilde\epsilon_d-\frac{J^2\Delta_0^2}{\omega-\tilde\epsilon_f}-\Sigma_0(\omega)},\\
\langle\langle f_\sigma|f_\sigma^\dagger\rangle\rangle &= \frac{1}{\omega-\tilde\epsilon_f-\frac{J^2\Delta_0^2}{\omega-\tilde\epsilon_d-\Sigma_0(\omega)}},
\end{aligned}\tag{20}$$

where $\tilde\epsilon_d=\epsilon_d+\lambda_d$, $\tilde\epsilon_f=\epsilon_f+\lambda_f$, and $\Sigma_0(\omega)=\omega\sum_k\frac{2\tilde V_0^2}{\omega^2-\hbar^2v_F^2k^2-A_k^2}$.

In the limit $\Delta_0\to0$, the impurity and the bound states are decoupled and the results reduce to those when $J=0$. When the spin exchange interaction exceeds a critical J_c, a nonzero order parameter Δ_0 appears and the Kondo peak near the chemical potential is expected to split. From the Green's functions $\langle\langle d_\sigma|d_\sigma^\dagger\rangle\rangle$, one obtains the self-consistent equation for the bound states,

$$\epsilon_f-\tilde\epsilon_d-\frac{J^2\Delta_0^2}{\epsilon_f-\tilde\epsilon_f}-\Sigma_0(\epsilon_f)=0.$$

Defining $\alpha(\omega)=[\omega-\tilde\epsilon_d-\mathrm{Re}\Sigma_0(\omega)](\omega-\tilde\epsilon_f)-J^2\Delta_0^2$ and $\beta(\omega)=\mathrm{Im}\Sigma_0(\omega)(\omega-\tilde\epsilon_f)$, the self-consistent equations are derived as

$$\begin{aligned}
-\frac{2}{\pi}\int_{-\infty}^{\mu}d\omega\frac{(\omega-\tilde\epsilon_f)\beta(\omega)}{\alpha(\omega)^2+\beta(\omega)^2}+b_d^2-1 &= 0,\\
-\frac{2}{\pi}\int_{-\infty}^{\mu}d\omega\frac{J^2\Delta_0^2\mathrm{Im}\Sigma_0(\omega)}{\alpha(\omega)^2+\beta(\omega)^2} &= 1,\\
-\frac{2}{\pi}\int_{-\infty}^{\mu}d\omega\frac{J\Delta_0\beta(\omega)}{\alpha(\omega)^2+\beta(\omega)^2}+\Delta_0 &= 0,\\
\frac{2}{\pi}\int_{-\infty}^{\mu}d\omega\frac{[(\omega-\tilde\epsilon_d)(\omega-\tilde\epsilon_f)-J^2\Delta_0^2]\beta(\omega)}{\alpha(\omega)^2+\beta(\omega)^2} &= \lambda_db_d^2,\\
\alpha(\epsilon_f) &= 0.
\end{aligned}\tag{21}$$

This set of equations can be solved numerically.

D. Self-screened Kondo effect

Figure 8 presents the effects of bound-state spin on the Kondo effect for different exchange interaction strength J. The chemical potential of the bulk of the TI is tuned into the conduction bands, so there is a Kondo peak near the chemical potential and the bound states are occupied by a single electron. When J exceeds a critical value J_c, the order parameter Δ_0 begins to increase from zero, then quickly to 1 with the increase of J. Figure 8(b) shows the density of states of the impurity as a function of energy for $J=0.0$, 0.04, and 0.08. With the increase of J, the resonance peak splits. The splitting of the Kondo peak increases with J. As a result, the density of states near $\tilde\epsilon_d$ reduces to a very small value, corresponding to the self-screening of the Kondo resonance.

It should be noted that the strength of exchange interaction between the impurity and the in-gap bound state is the key parameter of the predicted self-screened Kondo effect. The exchange strength should be evaluated subtly, for instance, from the first-principles calculation. Our calculation indicates that a small exchange interaction could make the Kondo effect break down.

Above we assumed that the bound states are singly-occupied in the large-U limit. If the Coulomb repulsion energy on the bound states is finite and the chemical potential is high enough, it is possible that the bound states are occupied by two electrons, and they form a singlet due to the Pauli exclusion principle. In this limit, the bound-state spin is decoupled from the impurity spin, and the Kondo effect originating from the interaction between the impurity spin and conduction electrons can recover.

An impurity- or vacancy- induced in-gap bound state is a special feature of TIs, which is absent in normal insulators. Therefore, the bound state may play an important role when the Kondo physics is considered in TIs. For a strong exchange interaction between impurity and in-gap bound state, the Kondo effect may be broken down when the chemical potential is tuned properly.

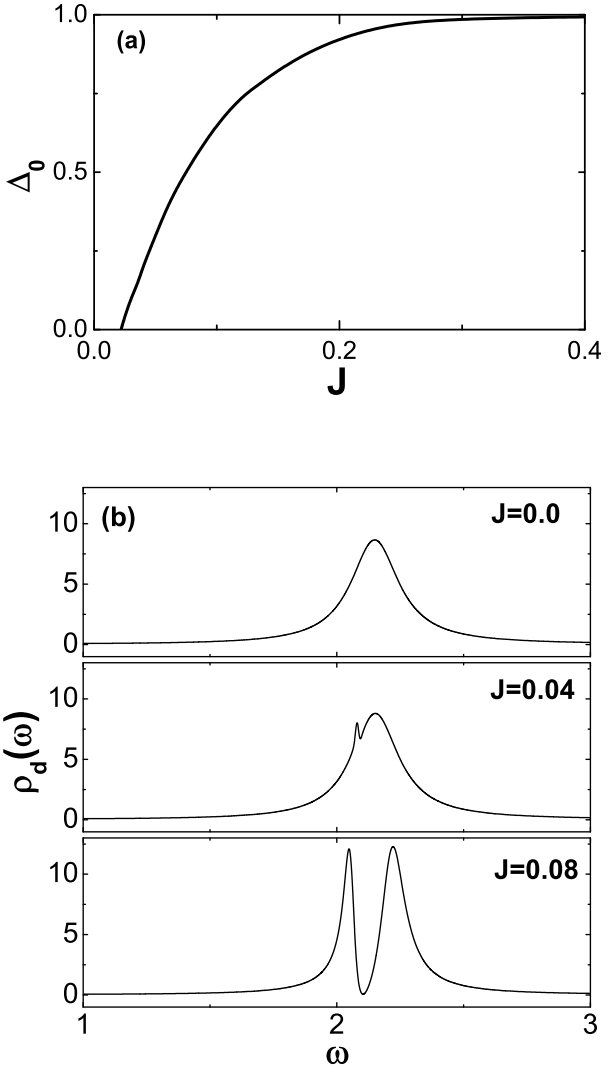

FIG. 8: (a) The order parameter Δ_0 as a function of J. Parameters: $\epsilon_d = 1.0$, $\mu = 2.0$, and $mB = 1.0$. (b) The density of states of the impurity for $J = 0.0$, 0.04, and 0.08.

Actually, several experiments have been performed to investigate the physical properties of magnetic impurity-doped topological materials, such as Mn-doped BiTe.[49] The self-screening effect is expected to be observed in these systems.

V. SUMMARY

In summary, we have studied the Kondo effect and the formation of in-gap bound states induced by an Anderson impurity coupled with the bulk states of topological insulators. It is demonstrated that the positions of the Kondo peak and bound states strongly depend on the topological properties, the chemical potential, and other parameters of the system. The behaviors of the resonance level in the bulk of TIs differ from those for simple metals and normal insulators. Due to the divergence of the density of states near the band edges, the mixed-valence regime is much broader in the band-inverted case, while it shrinks to a very narrow regime in the normal case. For the band-inverted case, the in-gap bound states and the Kondo resonance can coexist. However, only one of them exists in the normal insulators. When the impurity energy level is far away from the chemical potential, the in-gap bound states are very close to the band edges and can be considered as merging into the bulk. Furthermore, we show that a self-screening Kondo effect may be induced by taking the interaction between the impurity spin and bound-state spin into account.

Note added: while this manuscript was under review, we became aware of a work [50], wherein the scattering of dilute magnetic impurities placed on the surface of TIs is investigated.

This project was supported by the Research Grant Council under Grants No. HKU 7051/10P and No. HKUST3/CRF/09, the Foundation for Innovative Research Groups of the NSFC under Grant No. 61021061, the NSFC under Grants No. 11004022 and No. 61006081.

[1] M. Z. Hasan and C. L. Kane, Rev. Mod. Phys. **82**, 3045 (2010).
[2] X. L. Qi and S. C. Zhang, Rev. Mod. Phys. **83**, 1057 (2011).
[3] J. E. Moore, Nature (London) **464**, 194 (2010).
[4] H. Zhang, C. X. Liu, X. L. Qi, X. Dai, Z. Fang, and S. C. Zhang, Nat. Phys. **5**, 438 (2009).
[5] Y. L. Chen et al., Science **325**, 178 (2009).
[6] Y. Xia et al., Nat. Phys. **5**, 398 (2009).
[7] C. Wu, B. A. Bernevig, and S. C. Zhang, Phys. Rev. Lett. **96**, 106401 (2006).
[8] C. Xu and J. E. Moore, Phys. Rev. B **73**, 045322 (2006).
[9] Q. Liu, C. X. Liu, C. Xu, X. L. Qi, and S. C. Zhang, Phys. Rev. Lett. **102**, 156603 (2009).
[10] R. R. Biswas and A. V. Balatsky, Phys. Rev. B **81**, 233405 (2010).
[11] P. Roushan, J. Seo, C. V. Parker, Y. S. Hor, D. Hsieh, D. Qian, A. Richardella, M. Z. Hasan, R. J. Cava, and A. Yazdani, Nature **460**, 1106 (2009).
[12] T. Zhang, P. Cheng, X. Chen, J. F. Jia, X. Ma, K. He, L. Wang, H. Zhang, X. Dai, Z. Fang, X. C. Xie, and Q. K. Xue, Phys. Rev. Lett. **103**, 266803 (2009).
[13] Z. Alpichshev et al., Phys. Rev. Lett. **104**, 016401 (2010).
[14] Z. Alpichshev, R. R. Biswas, A. V. Balatsky, J. G. Analytis, J. H. Chu, I. R. Fisher, and A. Kapitulnik, Phys. Rev. Lett. **108**, 206402 (2012).
[15] A. M. Black-Schaffer and A. V. Balatsky, Phys. Rev. B **85**, 121103(R) (2012).
[16] R. Žitko, Phys. Rev. B **81**, 241414 (2010).

[17] M. T. Tran, and K. S. Kim, Phys. Rev. B **82**, 155142 (2010).
[18] Q. Liu and T. X. Ma, Phys. Rev. B **80**, 115216 (2009).
[19] W. Y. Shan, J. Lu, H. Z. Lu, and S. Q. Shen, Phys. Rev. B **84**, 035307 (2011).
[20] J. Lu, W. Y. Shan, H. Z. Lu and S. Q. Shen, New J. Phys. **13**, 103016 (2011).
[21] L. Andrew Wray, et al, Nat. Phys. **7**, 32 (2010).
[22] X. Y. Feng, W. Q. Chen, J. H. Gao, Q. H. Wang, and F. C. Zhang, Phys. Rev. B **81**, 235411 (2010).
[23] J. G. Checkelsky, Y. S. Hor, M. H. Liu, D. X. Qu, R. J. Cava, and N. P. Ong, Phys. Rev. Lett. **103**, 246601 (2009).
[24] K. Eto, Z. Ren, A. A. Taskin, K. Segawa, and Y. Ando, Phys. Rev. B **81**, 195309 (2010);
[25] Z. Ren, A. A. Taskin, S. Sasaki, K. Segawa, and Y. Ando, Phys. Rev. B **82**, 241306(R) (2010).
[26] D. X. Qu, Y. S. Hor, J. Xiong, R. J. Cava, and N. P. Ong, Science **329**, 821 (2010).
[27] H. Peng, K. Lai, D. Kong, S. Meister, Y. Chen, X. L. Qi, S. C. Zhang, Z. X. Shen, and Y. Cui, Nat. Mater. **9**, 225 (2010).
[28] A. V. Balatsky, I. Vekhter, and J. X. Zhu, Rev. Mod. Phys. **78**, 373 (2006).
[29] D. Withoff and E. Fradkin, Phys. Rev. Lett. **64**, 1835 (1990);
[30] C. Gonzalez-Buxton and K. Ingersent, Phys. Rev. B **57**, 14254 (1998).
[31] B. Dóra, Phys. Rev. B **71**, 075107 (2005).
[32] J. Ogura and T. Saso, J. Phys. Soc. Jpn. **62**, 4364 (1993).
[33] M. R. Galpin and D. E. Logan, Phys. Rev. B **77**, 195108 (2008).
[34] M. Zarea, S. E. Ulloa, and N. Sandler, Phys. Rev. Lett. **108**, 046601 (2012).
[35] R. Žitko and J. Bonča, Phys. Rev. B **84**, 193411 (2011).
[36] E. Eriksson, A. Ström, G. Sharma, and H. Johannesson, Phys. Rev. B **86**, 161103(R) (2012).
[37] H. Z. Lu, W. Y. Shan, W. Yao, Q. Niu, and S. Q. Shen, Phys. Rev. B **81**, 115407(2010).
[38] W. Y. Shan, H. Z. Lu, and S. Q. Shen, New J. Phys. **12**, 043048 (2010).
[39] S. Q. Shen, W. Y. Shan and H. Z. Lu, Spin **1**, 33 (2011).
[40] A. C. Hewson, The Kondo Problem to Heavy Fermions (Cambridge University Press, Cambridge, 1993).
[41] P. Coleman, Phys. Rev. B **29**, 3035 (1984).
[42] J. X. Zhu and C. S. Ting, Phys. Rev. B **63**, 020506 (2000).
[43] Z. G. Zhu and J. Berakdar, Phys. Rev. B **83**, 195404 (2011).
[44] K. Machida and F. Shibata, Prog. Theor. Phys. **47**, 1817 (1972).
[45] C. Chan and T. K. Ng, Phys. Rev. B **85**, 115207 (2012).
[46] B. A. Jones, C. M. Varma, and J. W. Wilkins, Phys. Rev. Lett. **61**, 125 (1988).
[47] R. López, R. Aguado, and G. Platero, Phys. Rev. Lett. **89**, 136802 (2002).
[48] I. Kuzmenko, Y. Avishai, and T. K. Ng, arXiv: 1303.0911.
[49] Y. S. Hor, P. Roushan, H. Beidenkopf, J. Seo, D. Qu, J. G. Checkelsky, L. A. Wray, D. Hsieh, Y. Xia, S. Y. Xu, D. Qian, M. Z. Hasan, N. P. Ong, A. Yazdani, and R. J. Cava, Phys. Rev. B, **81**, 195203 (2010).
[50] A. K. Mitchell, D. Schuricht, M. Vojta, and L. Fritz, Phys. Rev. B **87**, 075430 (2013)